Available online at www.sciencedirect.com
ScienceDirect
Trans. Nonferrous Met. Soc. China 33(2023) 938−950
Transactions of Nonferrous Metals Society of China
www.tnmsc.cn

Optimisation of extraction of valuable metals from waste LED via response surface method

Xu-yi WEI[1], Yong-feng GAO[2], Jun-wei HAN[1,2], Yong-wei WANG[1], Wen-qing QIN[1]

1. School of Minerals Processing and Bioengineering, Central South University, Changsha 410083, China;
2. Department of Chemical and Materials Engineering, University of Alberta, Edmonton T6G 1H9, Canada

Received 15 November 2021; accepted 27 April 2022

Abstract: The valuable metals were separated and extracted from waste light-emitting diodes (LEDs) by pyrolysis and leaching process. About 98.16% Ga and 99.54% Y were recycled from the LEDs after the pyrolysis by sieving process in advance. The effects of various leaching conditions on the extraction of Fe, Cu and Ag were investigated by single factor experiments and response surface method. About 90.15% Fe was selectively extracted from the waste LEDs by H_2SO_4 leaching without oxidant, and 99.55% Cu and 99.36% Ag were recovered from the iron leaching residue by acid leaching with the addition of HNO_3. The XRD and SEM−EDS analyses confirmed that the iron and copper were effectively extracted from the waste LEDs by the developed process.

Key words: acid leaching; metal recovery; response surface method; waste LEDs

1 Introduction

Light-emitting diodes (LEDs) are widely used in landscapes, vehicles and displays due to their advantages of high efficiency and carbon emission reduction [1−4]. These benefits have led to a rapid increase in the LED lighting market share, thus resulting in that a large number of waste LEDs will be generated [5]. Waste LEDs contain plenty of valuable metals, such as Ga, Y, Ag, and Cu, and are considered as an emerging urban mineral [6−8]. It is therefore of great economic and environmental importance to recover the valuable metals from waste LEDs.

The technologies for the recovery of valuable metals from waste LEDs can be summarised as physical separation, and hydrometallurgical and pyrometallurgical processes. CENCI et al [9] used electrostatic separation after griding to enrich 96.15% Ga and 95.20% Y in the nonconductor product and isolate 80.18% Au and 94.22% Ag in the conductor product, but Fe and Cu were not recovered. REUTER and van SCHAIK [10] optimized the recycling route for waste LEDs by using traditional Cu metallurgy techniques. However, the method ignored rare earth metals and rare metals due to their low grades. ZHAN et al [11,12] applied pyrolysis to releasing LED chips from packaging plastic in advance, and about 93.48% Ga and 95.67% In were recovered from the chips by vacuum metallurgy at 1373 K and 0.01−0.1 Pa for 60 min. However, the pyro-metallurgical process requires the strict conditions of high temperature and vacuum.

Hydrometallurgy is widely considered to be a green and high-efficiency method for metal recovery [13−15]. SWAIN et al [16,17] used Na_2CO_3 roasting followed by HCl leaching to treat the Ga dusts generated by the LED industry and optimized the process by using thermodynamic calculations. CHEN et al [18] used pressure leaching

Corresponding author: Jun-wei HAN, Tel: +86-13875815330, E-mail: hanjunwei2008@163.com
DOI: 10.1016/S1003-6326(23)66157-6

for the recovery of 98.46% Ga from waste LEDs. MAAREFVAND et al [19] obtained more than 90% Ga through roasting−leaching process after incineration. Some researchers had also used critical liquids, biohydrometallurgy and tribromide ionic liquids to recover rare metals, such as Ga and In, from waste LEDs [20−22]. Nevertheless, these methods are still in the laboratory research stage and have not been applied in the industry.

As mentioned previously, most of studies have focused on the recovery of some valuable metals from waste LEDs and there is no report on the comprehensive recovery of valuable metals from waste LEDs to our knowledge. Most researchers prefer to recover the rare or precious metals from waste LEDs and leaching residues, including Cu, Fe, and even Ag, in large amounts, leading to concerns over not only the economic loss but also the potential environmental threat [23−28]. Therefore, a novel process that combined pyrolysis and hydrometallurgy was developed to comprehensively recover valuable metals from waste LEDs. The aim of pyrolysis is to release valuable metals from encapsulated plastics. Ga and Y can be easily isolated from the pyrolysis residue by sieving process, because they are mainly distributed in the fine particle fraction (<630 μm) based on the mineralogical analysis. The large particle sample obtained is subjected to acid leaching for selectively extracting Fe, and the leaching reside is used to recover Cu and Ag by acid oxidative leaching.

In contrast to orthogonal experiments, the response surface method provides an intuitive and accurate picture of the effect of each factor on results and can predict the range of response values under different conditions [29−31]. In this study, the response surface method was utilised to identify the optimal conditions for the leaching of Cu, Fe and Ag from waste LEDs after pyrolysis. The effects of experimental parameters, including leaching temperature, time, H_2SO_4 concentration and oxidant concentration, on the extraction of the metals were combined by Design-Expert 13. Additionally, the chemical composition and morphological changes of waste LEDs during the process were detected via inductively coupled plasma (ICP-OES), X-ray diffraction (XRD). and scanning electron microscopy (SEM) coupled with energy dispersive spectroscopy (EDS).

2 Experimental

2.1 Materials

The waste LEDs used in this study were supplied by a lighting company in Shenzhen, China. A structural diagram of LEDs and a photo of waste LEDs are shown in Fig. S1 in Supporting Information (SI). LEDs consist of a plastic support, epoxy resin, chips, phosphor, and pins. The pins mainly include cathodes and anodes, which contain plenty of Cu and Fe. In addition, the chips were connected with the pins by silver glue, which is an important secondary silver resource. Table S1 in SI gives the main metal composition of the waste LED. It contains 45.27% Fe, 10.80% Cu, and minor rare metals (0.26% Ag and 0.33% Ga). Unless otherwise stated, the reagents used in the experiments were of analytical grade. Ultrapure water was used in all the experiments.

2.2 Methods

A flow diagram of the developed process for comprehensive recovery of waste LEDs is shown in Fig. S2 in SI. For each pyrolysis test, 20 g of waste LED was taken and placed into a crucible, which was then placed into the pyrolysis furnace. The pyrolysis furnace was fed with N_2 as a protective gas and connected to a pyrolysis oil absorption unit, wherein the gas produced by the pyrolysis was collected in gas bags. The pyrolysis conditions were set as 550 °C for 60 min. After pyrolysis, the slags were cooled to room temperature. The rare metals and metal pins were separated by using a 630 μm sieve. The metal pins constituted 75.28% of the waste LED pyrolysis slag, which contained 17.92% Cu, 73.75% Fe and 3886.43 g/t Ag after analyzing by ICP-OES. The grades of Ga and Y in the fine fraction (<630 μm) were 1.62% and 3.25%, respectively. It was calculated that 98.16% Ga and 99.54% Y were separated into the fine sample by the sieving process. The waste LED metal pins obtained after the pyrolysis were detected by SEM−EDS analysis (Fig. S3 in SI). It was subjected to acid leaching for the extraction of Fe, Cu, and Ag in the subsequent process. For each test, 10 g of the metal pins were placed in a glass beaker with pre-prepared leach solution, which was heated in a constant-temperature water bath and subjected to mechanical stirring. After leaching, the residue was

separated from the leachate through vacuum filtration and washed with ultrapure water several times. The leachates and the washing water were diluted to a constant volume using a volumetric flask and analysed for Cu, Fe, and Ag contents by ICP-OES. The further separation and recovery of rare metals including Ga and Y will be carried out using ionic adsorption with advanced functional materials in the future.

The contents of Cu, Fe, and Ag were analyzed with ICP-OES (5100 USA Agilent Technologies) after the samples were digested with a mixture of concentrated HCl and HNO_3 (3:1, v/v). The phase compositions of the samples were determined by using XRD (X' Pert3 Powder X-ray diffractometer Netherlands PANalytical B.V.). The morphological changes of the leaching residues were investigated by SEM (Quanta FEG250) coupled with EDS (Genesis XM2). All these techniques were conducted in accordance with the ISO standard. The response surface experiments for identifying the optimal leaching conditions were designed with the Box-Behnken module of Design-Expert 13 software. The leaching model is represented by Eq. (1), where R represents the response value and is also known as the extraction rate, and A, B and C represent the influencing factors. The factors involved in this study are listed in Tables S2 and S3 in SI. Additionally, the coefficients of the linear, quadratic and interaction effects are represented by β.

$$R=\beta_0+\beta_1A+\beta_2B+\beta_3C+\beta_{12}AB+\beta_{13}AC+\beta_{23}BC+\beta_{11}A^2+\beta_{22}B^2+\beta_{33}C^2 \quad (1)$$

3 Results and discussion

3.1 φ−pH diagrams

The metal−H_2O systems were used as a guide for determining the pH and potential values of the leaching conditions. The φ−pH diagrams of Fe−H_2O, Cu−H_2O, and Ag−H_2O systems at 25 °C were generated by FactSage 8.0 (Fig. 1). As shown in Fig. 1(a), Fe can be gradually oxidized into Fe(II) and Fe(III) as the potential is increased. The potential required for the oxidisation of Fe decreases as the pH is increased. In acidic solutions, the conditions for the conversion of Fe to Fe^{2+} are pH < 5.5 and −0.40 V < φ < 0.77 V. Figure 1(b) shows that the conditions for the conversion of Cu to Cu^{2+} are pH < 3.95 and φ > 0.337 V. As depicted in Fig. 1(c), the extraction of Ag requires a high potential of φ > 0.80 V and pH < 6.20. As discussed above, Fe in the waste LED metal pins can be extracted with H_2SO_4 solution without any oxidant, and the extraction of Cu and Ag through acid leaching requires an oxidative condition.

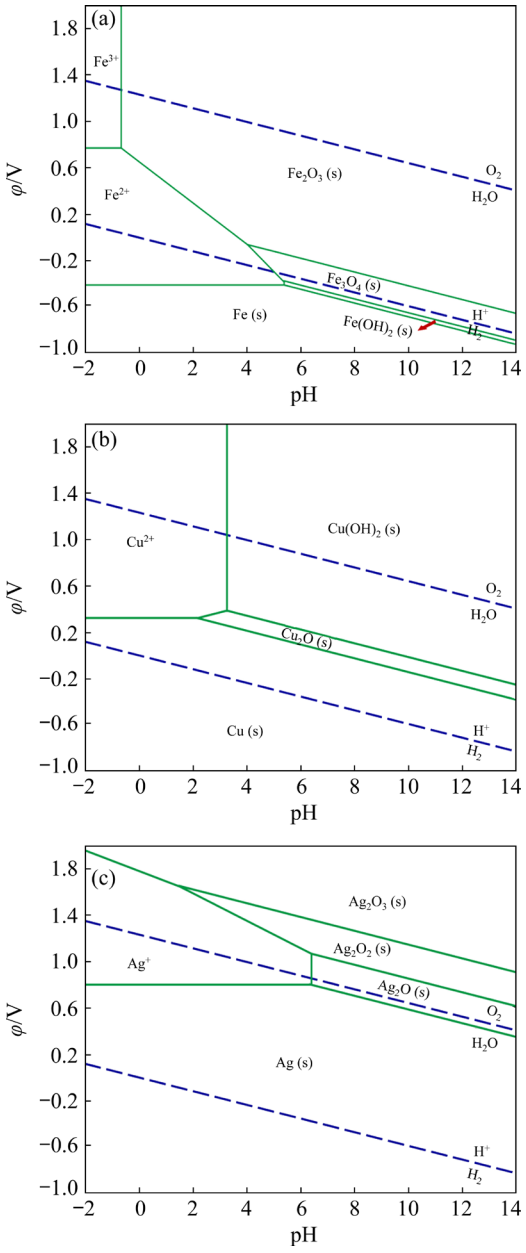

Fig. 1 φ−pH diagrams of Fe−H_2O (a), Cu−H_2O (b), and Ag−H_2O (c) systems at 25 °C

3.2 Selectively leaching Fe from waste LEDs

3.2.1 Single factor experiments for Fe leaching

Single-factor experiments were performed to investigate the effects of H_2SO_4 concentration, leaching temperature and time on the selective leaching of Fe from the waste LEDs at the liquid/solid ratio of 7 mL/g (Fig. 2). As shown in Fig. 2(a),

leaching temperature has a more significant influence on the extraction of Fe leaching than the other factors. The extraction of Fe increases rapidly with increasing the temperature, from 40 to 80 °C, above which the extraction of Fe has no obvious change as the temperature further increases. Meanwhile, the extractions of Cu and Ag are less than 1% when the leaching temperature is below 80 °C, implying that the selective extraction of Fe is feasible. Figure 2(b) illustrates the effect of H_2SO_4 concentration on leaching. The extraction of Fe gradually increases from 68.18% to 83.81% when the acid concentration is increased from 1.0 to 2.5 mol/L, above which it increases slightly with the further increase in H_2SO_4 concentration. However, the extraction of Cu and Ag will significantly increase with further increasing the acid concentration. As a result, 2.5 mol/L H_2SO_4 is considered as the optimal acid concentration. As seen from Fig. 2(c), the extraction of Fe gradually increases as the leaching time is extended from 1.0 to 8.0 h. Thereafter, it has no significant variation with the further increase in time [32]. Approximately 88.34% Fe is extracted from the waste LEDs through the leaching with 2.5 mol/L H_2SO_4 at 80 °C for 8 h, while the extractions of Cu and Ag are less than 1%.

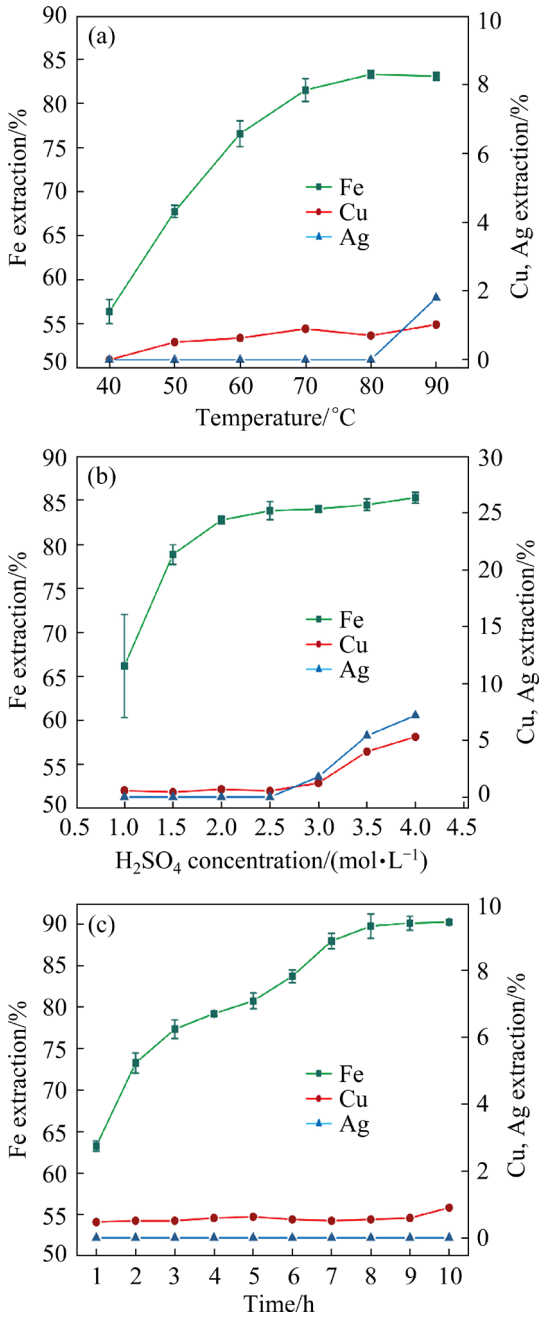

Fig. 2 Effects of leaching conditions on extraction of Fe: (a) Leaching temperature; (b) H_2SO_4 concentration; (c) Leaching time

3.2.2 Statistical analysis and model fitting for Fe leaching

Through the single-factor experiments, the response surface experiments would provide the optimal option with the maximum Fe extraction and the minimum time and economic costs. A total of 17 sets of conditional experiments were generated with the help of Design Expert 13 software (Table 1). Simultaneously, the extraction of Fe was fitted to a multivariate quadratic equation (Eq. (2)).

$$R(\mathrm{Fe})=42.92875+0.869250A+10.61250B-7.01875C+0.2AB+0.049AC+0.505CB-0.00916A^2-6.095B^2+0.36625C^2 \quad (2)$$

The optimization model for Fe leaching was subjected to the significance analysis and testing (Table 2). The F-value of the regression model is 40.62 with a P-value of 0.0001, which is less than 0.05, indicating that the resulting Fe leaching model is highly significant. By contrast, the F-value of the misfit term is 0.9306 with a P-value of 0.5037, which is greater than 0.05, implying that the misfit of the model is not significant. Consequently, the model is a good predictor of the effects of temperature (A), acid concentration (B), and leaching time (C) on the extraction of Fe within the regression range investigated. The P-values for the primary terms A, B and C in the model are all less than or equal to 0.0001 and those for the secondary terms AB, A^2 and B^2 are less than 0.05. These results indicate that these influencing factors have a profound and significant effect on the leaching of Fe. The order of the significance of the influence factors is $A > C > B > B^2 > AB > A^2$, based on the magnitudes of the F-values.

Table 1 Response surface design scheme and experimental results of Fe extraction from waste LEDs

No.	*A*/°C	*B*/(mol·L^{-1})	*C*/h	Fe extraction/%
1	80	2.5	7	87.25
2	70	1.5	6	78.47
3	70	2.5	8	86.96
4	80	1.5	7	81.86
5	60	2.5	7	78.5
6	70	2	7	84.91
7	70	2	7	83.33
8	60	1.5	7	77.11
9	60	2	6	77.42
10	70	2	7	83.31
11	80	2	8	89.7
12	80	2	6	82.87
13	70	1.5	8	82.31
14	70	2	7	83.38
15	60	2	8	82.29
16	70	2.5	6	82.11
17	70	2	7	83.17

Table 2 Analysis of variance and significance for Fe leaching regression model

Source	Sum of square	df	Mean square	*F*-value	*P*-value
Model	186.62	9	20.74	40.62	< 0.0001
A	86.86	1	86.86	170.16	< 0.0001
B	28.39	1	28.39	55.61	0.0001
C	51.97	1	51.97	101.81	< 0.0001
AB	4	1	4	7.84	0.0265
AC	0.9604	1	0.9604	1.88	0.2125
BC	0.255	1	0.255	0.4996	0.5025
A^2	3.53	1	3.53	6.92	0.0338
B^2	9.78	1	9.78	19.15	0.0032
C^2	0.5648	1	0.5648	1.11	0.3278
Residual	3.57	7	0.5104		
Lack of fit	1.47	3	0.4896	0.9306	0.5037
Pure error	2.1	4	0.5261		
Cor total	190.2	16			

As presented in Fig. 3(a), the extraction of Fe predicted by the model was compared with the actual extraction rate. It clearly shows that the actual values are concentrated on a straight line. Figure 3(b) indicates that the residuals of Fe extraction and the predicted values are within manageable limits. Therefore, the response surface method applied to model Fe extraction is reliable over the entire regression range.

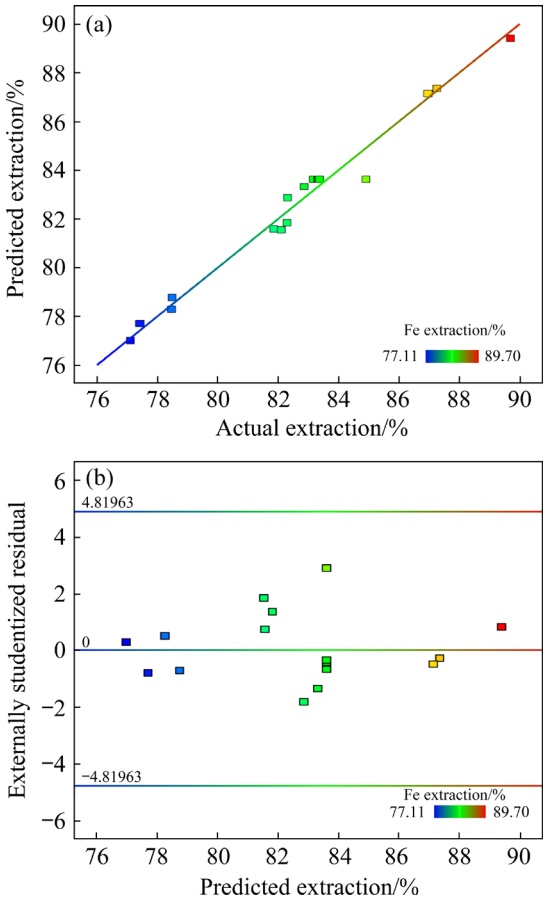

Fig. 3 Relation between predicated and actual extraction of Fe leaching: (a) Predicted vs actual extraction; (b) Residual and predicted extraction distribution

3.2.3 Optimization for Fe leaching

Three-dimensional response surfaces and contours were drawn to investigate the interactions of temperature, H_2SO_4 concentration and leaching time on the extraction of Fe (Figs. 4 and S4 (in SI)). The colours represent different extraction rates, and the change in colour from blue to green and red indicates that the extraction rate gradually increases. Figure 4(a) depicts that with the increase in temperature, the extraction of Fe increases rapidly for various H_2SO_4 concentration, especially for 3.5 mol/L H_2SO_4, suggesting that leaching temperature plays an important in the leaching of Fe. Figure S4(a) (in SI) shows that the contour lines are more intensive in the temperature direction than

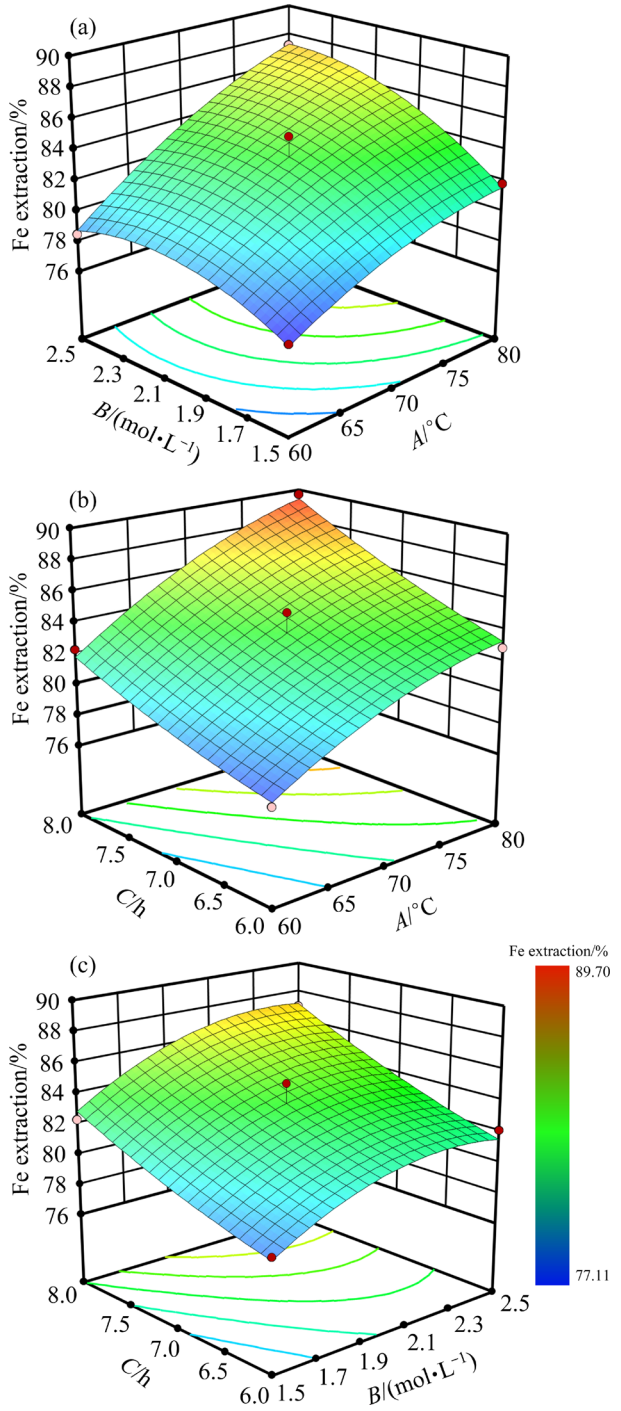

Fig. 4 Response surface of Fe leaching: (a) Effect of temperature on acid concentration; (b) Effect of temperature on time; (c) Effect of acid concentration on time

that in the acid concentration direction, indicating that the temperature has a more significant effect on the extraction of Fe. Figure 4(b) shows that both leaching time and temperature are critical factors on the extraction of Fe, and the temperature has a more pronounced effect than leaching time, which can be further proved by the contour line distribution (Fig. S4(b) in SI). Figure 4(c) indicates that the extraction of Fe increases with increasing the acid concentration and leaching time, and the time plays a more important influence on the leaching, compared with H_2SO_4 concentration, which has been proved by Fig. S4(c) in SI. In conclusion, the significance of these factors on the extraction of Fe follows the order: temperature > time > H_2SO_4 concentration. The results are consistent with the previous *F*-value ranking results.

Thanks to the optimization of iron leaching with response surface method, it is predicted that about 89.97% Fe can be extracted from the waste LEDs via acid leaching under the conditions of 80 °C of temperature, 2.36 mol/L H_2SO_4 concentration, 7 mL/g of liquid-to-solid ratio, and 7.76 h of leaching time. The confirmation experiments have proved that the actual extraction of Fe is 90.15%, which is in good agreement with the predicted result.

3.3 Oxidative leaching of Cu and Ag

3.3.1 Single factor experiments for leaching of Cu and Ag

The effects of leaching temperature, H_2SO_4 concentration, and oxidant dosage on the leaching of Cu and Ag were investigated. The liquid/solid ratio was fixed at 10 mL/g. Figure 5(a) shows that the leaching rates of Cu and Ag increase markedly as the leaching time is increased from 1 to 5 h, after which the extraction of Cu increases slightly but that of Ag still increases significantly. When the time is 5 h, the extractions of Cu and Ag reach 92.58% and 88.00%, respectively. This reveals that Ag is more difficult to be dissolved in the leaching solution. It is seen from Fig. 5(b) that increasing the temperature can enhance the leaching of Cu and Ag, and it has a more important influence on the extraction of Ag. As shown in Fig. 5(c), the extraction of Cu and Ag gradually increases with increasing H_2SO_4 concentration from 2.0 to 3.5 mol/L, above which they have no significant increase with further increasing the concentration. It is found from Fig. 5(d) that the addition of HNO_3 has a positive effective on the leaching, especially for Ag leaching [33−37]. The extractions of Cu and Ag are as high as 98.55% and 92.25%, respectively, when the dosage of HNO_3 is 60 g/L.

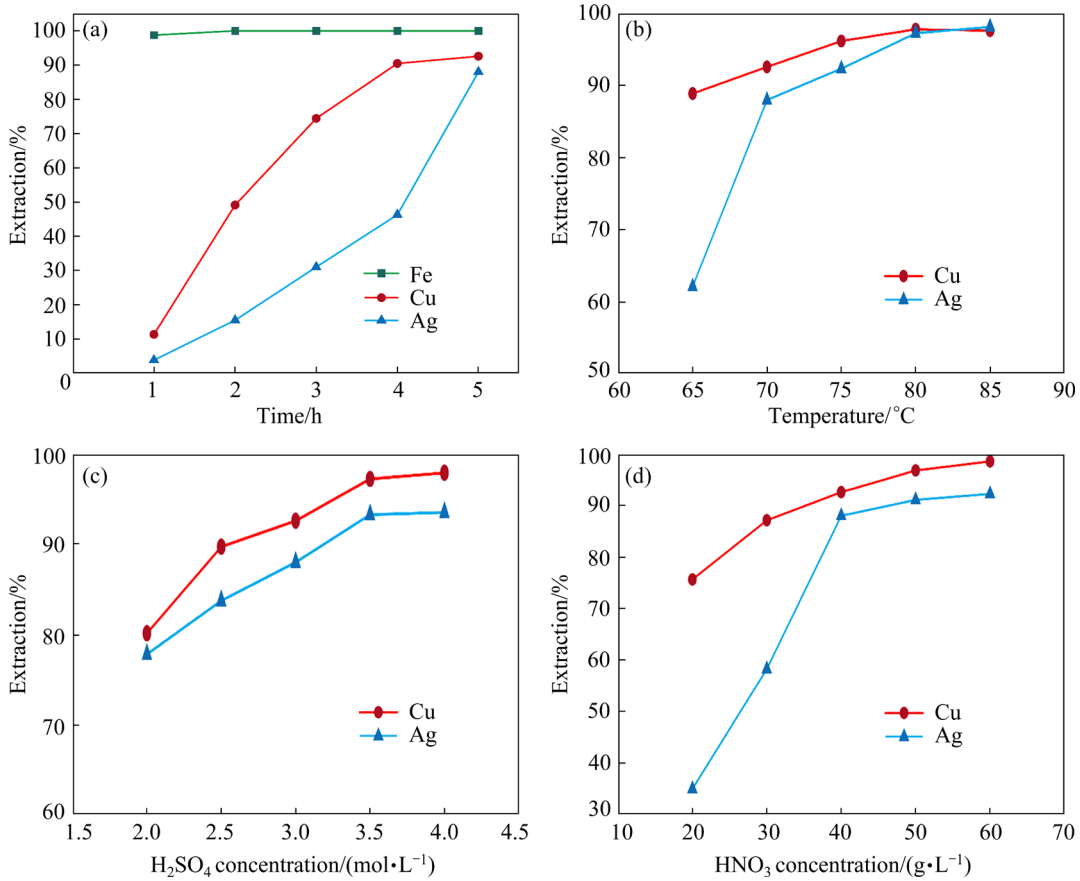

Fig. 5 Effects of leaching conditions on extraction of Cu and Ag: (a) Leaching time; (b) Temperature; (c) H_2SO_4 concentration; (d) HNO_3 concentration

3.3.2 Statistical analysis and model fitting for leaching of Cu and Ag

The response surface method was applied to further optimizing the experiments to obtain the most cost-effective leaching conditions for Cu and Ag. The interactions of H_2SO_4 concentration, oxidant concentration, and leaching temperature on the extraction of Cu and Ag were investigated on the basis of the results of the single-factor experiments. The results are provided in Table 3, and the multivariate quadratic equations for the leaching extractions of Cu and Ag are presented by Eqs. (3) and (4), respectively.

$$R(\text{Cu})=-229.26250+3.45260A+65.05100B+2.92975D-0.392AB-0.0084AD-0.182DB-0.01036A^2-3.676B^2-0.01434D^2 \quad (3)$$

$$R(\text{Ag})=-347.84625+3.58895A+91.082B+5.48563D-0.493AB-0.0149AD-0.3305DB-0.00726A^2-5.262B^2-0.02848D^2 \quad (4)$$

The results of the significance analysis and test of the optimization models for Cu and Ag leaching are shown in Tables 4 and 5, respectively. The

Table 3 Response surface design scheme and experimental results of Cu and Ag extraction from waste LEDs

No.	*A*/ °C	*B*/ (mol·L^{-1})	*D*/ (g·L^{-1})	Cu extraction/%	Ag extraction/%
1	75	2.5	50	93.63	91.74
2	85	2.5	50	98.32	97.88
3	80	3.5	40	94.96	92.1
4	75	3	40	93.36	89.06
5	80	2.5	60	98.89	98.35
6	80	3	50	98.77	98.66
7	80	3	50	98.57	98.53
8	80	2.5	40	90.5	84.59
9	80	3	50	98.82	97.89
10	80	3	50	97.35	96.01
11	80	3	50	98.33	97.59
12	80	3	60	98.74	98.26
13	75	3	60	98.02	97.09
14	75	3.5	50	98.79	98.3
15	85	3	60	99.15	98.89
16	80	3.5	60	99.71	99.25
17	85	3	40	95.45	92.67

* *D* represents HNO_3 concentration

F-values of the regression models for the leaching of Cu and Ag from the iron leaching residue are17.47 and 20.28, respectively, with *P*-values of 0.0005 and 0.0003, which are considerably less than 0.05, indicating that the Cu and Ag leaching models are highly significant. The *F*-values of the misfit terms are 2.93 and 1.73 respectively, with *P*-values of 0.1628 and 0.2986 that are greater than 0.05, indicating that the misfitting of the models is not significant. Therefore, the models can predict the effects of temperature (*A*), H_2SO_4 concentration (*B*), and oxidant concentration (*D*) well within the regression range. Notably, analogous to that in the Fe leaching model, the order of influence between factors can be found in the leaching models for Cu and Ag. The *P*-values for the primary term *D* in the Cu leaching model are less than 0.0001 and those for the secondary terms *AB*, D^2, and B^2 are less than or approach 0.05, implying that these factors have significant effect on Cu leaching. The *F*-values reveal that the order of significance is $D > D^2 > AB > B^2$. The order of significance for Ag leaching model is determined as $D > D^2 > BD$ by using the same method. As predicted, the concentration of the oxidant has the most pronounced effect on the extraction of Cu and Ag.

Table 4 Analysis of variance and significance for Cu leaching regression model

Source	Sum of square	df	Mean square	*F*-value	*P*-value
Model	103.83	9	11.54	17.47	0.0005
A	7.92	1	7.92	11.99	0.0105
B	12.85	1	12.85	19.46	0.0031
D	61.72	1	61.72	93.47	< 0.0001
AB	3.84	1	3.84	5.82	0.0466
AD	0.7056	1	0.7056	1.07	0.3357
BD	3.31	1	3.31	5.02	0.0601
A^2	0.2824	1	0.2824	0.4277	0.534
B^2	3.56	1	3.56	5.39	0.0533
D^2	8.66	1	8.66	13.11	0.0085
Residual	4.62	7	0.6603		
Lack of fit	3.18	3	1.06	2.93	0.1628
Pure error	1.44	4	0.3611		
Cor total	108.45	16			

Table 5 Analysis of variance and significance for Ag leaching regression model

Source	Sum of square	df	Mean square	*F*-value	*P*-value
Model	270.02	9	30	20.28	0.0003
A	16.79	1	16.79	11.35	0.0119
B	25.31	1	25.13	16.99	0.0044
D	164.98	1	164.98	111.52	< 0.0001
AB	6.08	1	6.08	4.11	0.0823
AD	2.22	1	2.22	1.5	0.2602
BD	10.92	1	10.92	7.38	0.0299
A^2	0.1188	1	0.1188	0.0803	0.7851
B^2	7.29	1	7.29	4.93	0.0619
D^2	34.15	1	34.15	23.08	0.002
Residual	10.36	7	1.48		
Lack of fit	5.85	3	1.95	1.73	0.2986
Pure error	1.444.51	4	1.13		
Cor total	280.38	16			

The model-predicted values for the extraction of Cu and Ag are compared with the actual data in Figs. 6(a) and (c). The graphs illustrate that the actual values are concentrated around a straight line. Figures 6(b) and (d) show that the residuals of the extraction of Cu and Ag are within a manageable range from the predicted values. Therefore, the models used by the response surface method to simulate the extraction of Cu and Ag are reliable over the entire range of regression areas.

3.3.3 Optimization for leaching of Cu and Ag

The three-dimensional response surfaces and contours are plotted in Figs. 7 and S5 to consider the interactions between factors. Compared with the other factors, oxidant concentration has a more pronounced effect on the extraction of Cu and Ag. In particular, when HNO_3 concentration was 60 g/L, over 97% of Cu and Ag are extracted from the residue. The Cu leaching model in Figs. 7(a) and S5(a) (in SI) shows that acid concentration has a more significant effect on the extraction of Cu than the temperature. By contrast, the Ag leaching model provided in Figs. 7(d) and S5(d) (in SI) illustrates that H_2SO_4 concentration and temperature have a comparable effect on the extraction of Ag. These results are consistent with the findings of the statistical tests for the extraction of Cu and Ag. The optimization of Cu and Ag leaching with response

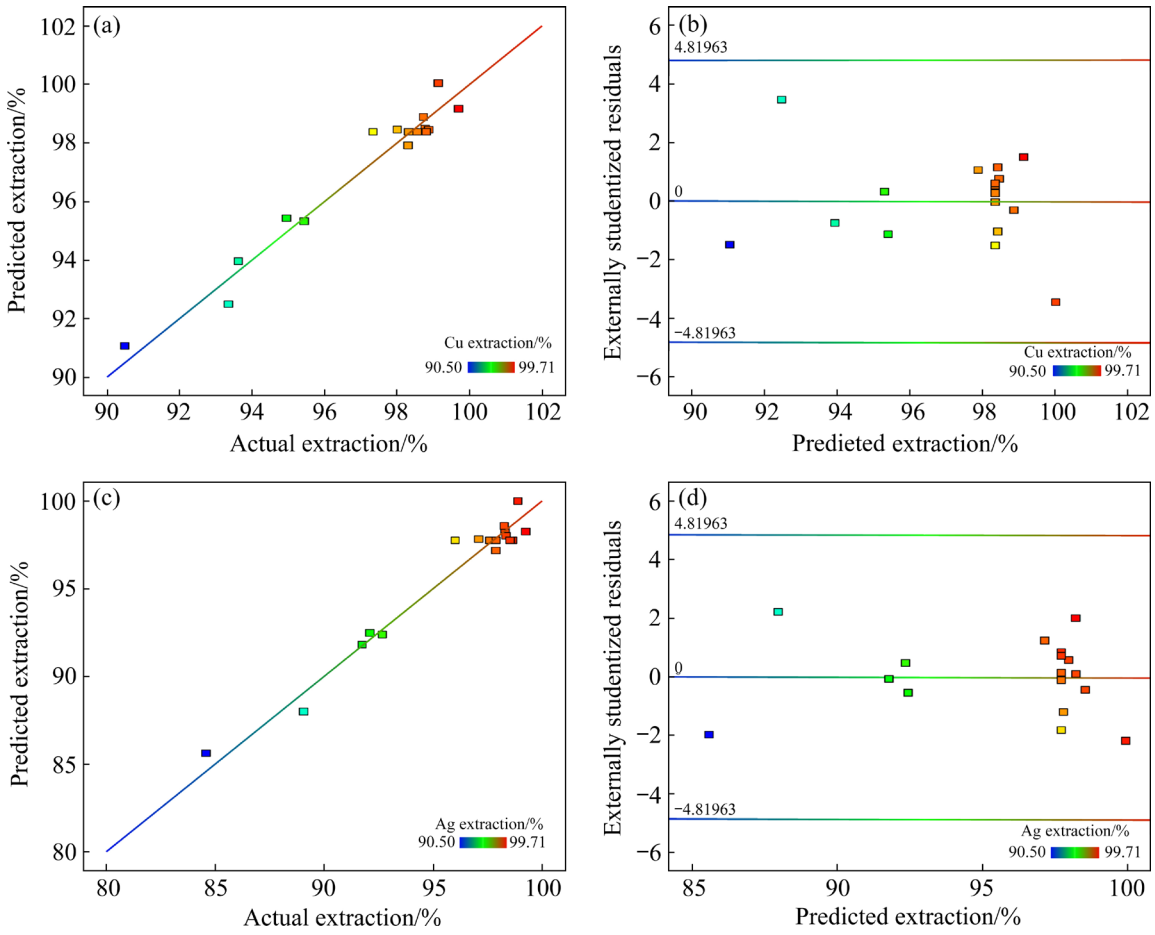

Fig. 6 Relations between predicated and actual extraction of Cu (a, b) and Ag (c, d) leaching: (a, c) Predicted vs actual extraction; (b, d) Residual and predicted extraction distribution

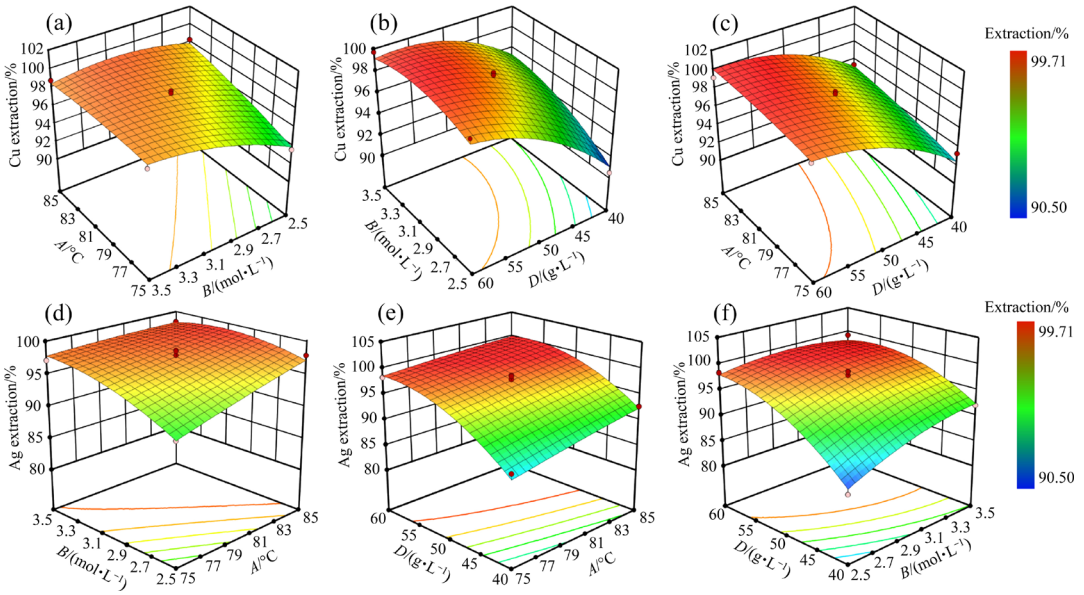

Fig. 7 Response surface of Cu and Ag leaching: (a) Effect of temperature and H_2SO_4 concentration on Cu leaching; (b) Effect of HNO_3 concentration and H_2SO_4 concentration on Cu leaching; (c) Effect of HNO_3 concentration and temperature on Cu leaching; (d) Effect of temperature and H_2SO_4 concentration on Ag leaching; (e) Effect of HNO_3 concentration and temperature on Ag leaching; (f) Effect of HNO_3 concentration and H_2SO_4 concentration on Ag leaching

surface method results in the maximum extraction rates of 99.79% Cu and 99.61% Ag at 80.4 °C, 3.1 mol/L H_2SO_4, 58.32 g/L HNO_3, and 10 mL/g liquid/solid ratio, 5 h. These above conditions are adopted for the experiments, and the actual leaching rates obtained are 99.55% Cu and 99.36% Ag, which are in accordance with the predicted results.

3.4 Phase transformation

The phase transformation of waste LEDs during the process was investigated and the XRD patterns of the pyrolysis residue, iron leaching residue, and Cu−Ag leaching residue are presented in Fig. 8. It is found from Fig. 8(a) that the pyrolysis residue is mainly composed of Fe, Cu, and TiO_2. Fe is selectively leached out by the first-stage leaching and the iron leaching residue primarily contains Cu, TiO_2, and $PbSO_4$ (Fig. 8(b)), which is generated during the leaching process through the reaction of Pb with H_2SO_4. The final residue is mainly composed of TiO_2 and $PbSO_4$, implying that Cu is extracted from the iron leaching residue. The silver phases are not detected by XRD due to too low content.

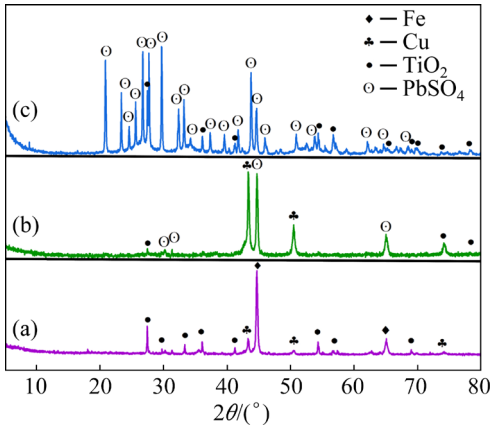

Fig. 8 XRD patterns of waste LEDs: (a) Pyrolysis residue; (b) Iron leaching residue; (c) Cu and Ag leaching residue

3.5 Morphology changes

The leaching residues were further analyzed by SEM−EDS to reveal the morphological changes during the process (Fig. 9). Correspondingly, the pyrolysis residue was analyzed as well (Fig. S3 in SI). The metal pins in the pyrolysis residue are larger than 700 μm in size, and Cu and Ag are found

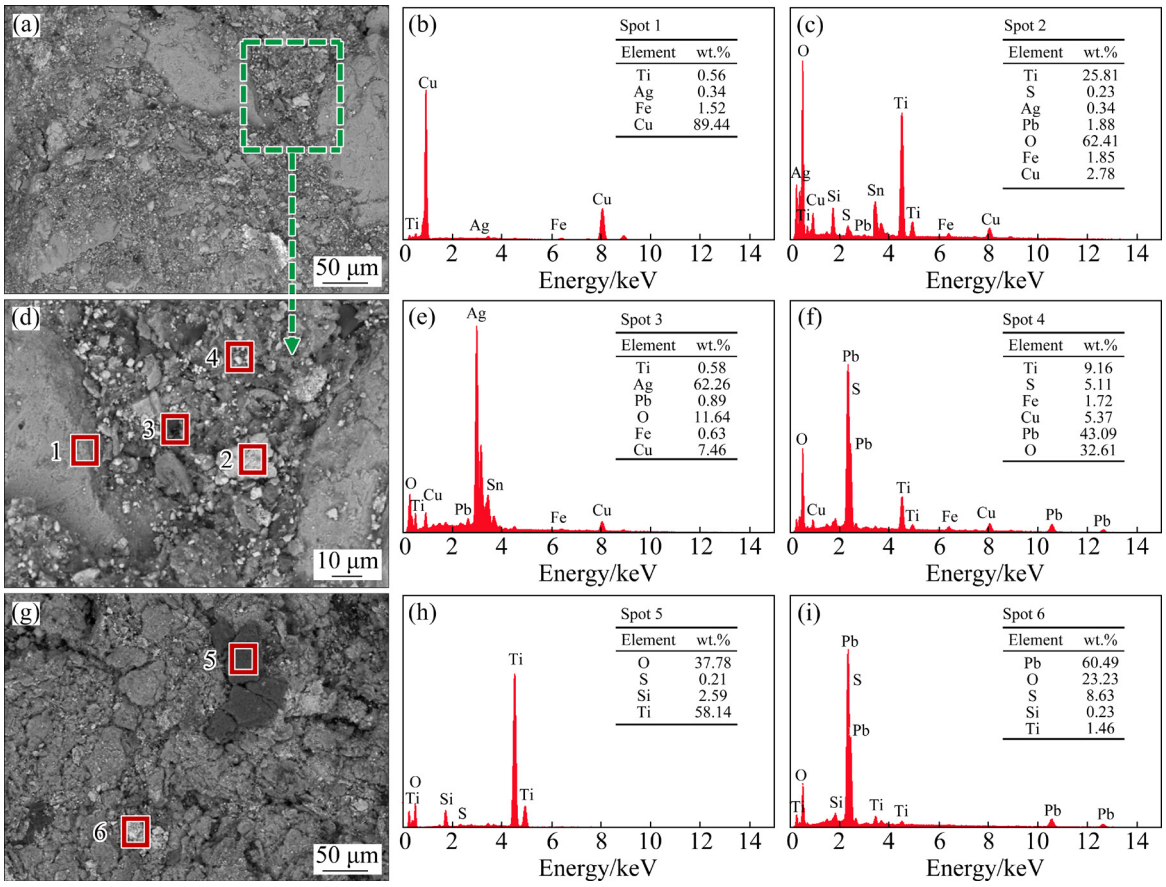

Fig. 9 SEM images (a, d, g) and EDS results (b, c, e, f, h, i) of leaching residues of waste LED

on the surfaces of metal pins with minor of TiO_2. As illustrated in Figs. 9(a) and (d), the surface of the leaching residue is rougher than that of the metal pins and exhibits obvious signs of erosion caused by Fe dissolution. In addition to Cu and Ag, some bright fine $PbSO_4$ particles (Spot 4) are presented in the iron leaching residue. After Cu and Ag leaching, the porosity of the leachate surface is increased, while the particle size is decreased to approximately 50 μm (Fig. 9(g)). The SEM−EDS results indicate that the resulting residue is mainly composed of TiO_2 and $PbSO_4$ as shown in Figs. 9(h) and (i). This is consistent with Fig. 8.

4 Conclusions

(1) About 90.15% Fe was selectively extracted from the waste LEDs after pyrolysis by acid leaching under the optimal conditions: 80 °C of temperature, 2.36 mol/L of H_2SO_4 concentration, 7 mL/g of liquid/solid ratio, and 7.76 h of leaching time. These leaching conditions have an important effect on the extraction of Fe, and the significance order is temperature > leaching time > H_2SO_4 concentration.

(2) Approximately 99.55% Cu and 99.36% Ag were extracted from the iron leaching residue under the optimal conditions: 80.4 °C of temperature, 3.1 mol/L of H_2SO_4 concentration, 58.32 g/L of HNO_3 concentration, 10 mL/g of liquid/solid ratio, and 5 h of leaching time. HNO_3 concentration has the most pronounced effect on the extraction of Cu and Ag.

(3) The XRD results indicated that the waste LEDs after the pyrolysis are mainly composed of Fe, Cu and TiO_2, the iron leaching residue primarily contains Cu, TiO_2 and $PbSO_4$, and the Cu−Ag leaching resides are mainly composed of TiO_2 and $PbSO_4$. This demonstrates that Fe and Cu are effectively extracted from the waste LEDs, which is further confirmed by SEM−EDS analysis.

(4) About 98.16% Ga and 99.54% Y could be isolated from the waste LEDs after the pyrolysis via a sieving process. The fine particle samples (<630 μm) obtained are rich in Ga and Y elements, which will be recovered by ionic adsorption with advanced functional materials in the future.

Acknowledgments

The authors are grateful for the financial support from the Natural Science Foundation of Hunan Province, China (No. 2021JJ20062), Innovation Driven Project of Central South University, China (No. 2020CX038), High-tech Industry Science and Technology Innovation Leading Project of Hunan Province, China (No. 2022GK4058), Landmark Innovation Demonstration Project of Hunan Province, China (No. 2019XK2304), the National Key R&D Program of China (No. 2019YFC1907301), and China Scholarship Council (No. 202006375018).

Supporting Information

Supporting information in this paper can be found at: http://tnmsc.csu.edu.cn/download/22-0938-2021-1468-supporting_information.pdf.

References

[1] YAN Fei, DEMIR H V. LEDs using halide perovskite nanocrystal emitters [J]. Nanoscale, 2019, 11(24): 11402−11412.

[2] JIANG Ai-li, ZUO Jin-hua, ZHENG Qiu-li, GUO Lei, GAO Li-pu, ZHAO Shu-gang, WANG Qing, HU Wen-zhong. Red LED irradiation maintains the postharvest quality of broccoli by elevating antioxidant enzyme activity and reducing the expression of senescence-related genes [J]. Scientia Horticulturae, 2019, 251: 73−79.

[3] NARDELLI A, DEUSCHLE E, de AZEVEDO L D, PESSOA J L N, GHISI E. Assessment of Light Emitting Diodes technology for general lighting: A critical review [J]. Renewable and Sustainable Energy Reviews, 2017, 75: 368−379.

[4] TSAI C Y. Design of free-form reflector for vehicle LED low-beam headlamp [J]. Optics Communications, 2016, 372: 1−13.

[5] REBELLO R Z, LIM M T W D C, YAMANE L H, SIMAN R R. Characterization of end-of-life LED lamps for the recovery of precious metals and rare earth elements[J]. Resources, Conservation & Recycling, 2020, 153: 104557.

[6] LIM S R, KANG D, OGUNSEITAN O A, SCHOENUNG J M. Potential environmental impacts of light-emitting diodes (LEDs): Metallic resources, toxicity, and hazardous waste classification [J]. Environmental Science & Technology, 2011, 45(1): 320−327.

[7] LIM S R, KANG D, OGUNSEITAN O A, SCHOENUNG J M. Potential environmental impacts from the metals in incandescent, compact fluorescent lamp (CFL), and light-emitting diode (LED) bulbs [J]. Environmental Science & Technology, 2013, 47(2): 1040−1047.

[8] CENCI M P, DAL BERTO F C, SCHNEIDER E L, VEIT H M. Assessment of LED lamps components and materials for a recycling perspective [J]. Waste Management, 2020, 107: 285−293.

[9] CENCI M P, DAL BERTO F C, CAMARGO P S S, VEIT H M. Separation and concentration of valuable and critical materials from wasted LEDs by physical processes [J]. Waste

Management, 2021, 120: 136−145.

[10] REUTER M A, van SCHAIK A. Product-centric Simulation-based design for recycling: Case of LED lamp recycling [J]. Journal of Sustainable Metallurgy, 2015, 1: 4−28.

[11] ZHAN Lu, XIA Fa-fa, YE Qiu-yu, XIANG Xi-shu, XIE Bing. Recycle gallium and arsenic from GaAs-based E-wastes via pyrolysis–vacuum metallurgy separation: Theory and feasibility [J]. ACS Sustainable Chemistry & Engineering, 2018, 6(1): 1336−1342.

[12] ZHAN Lu, XIA Fa-fa, YE Qiu-yu, XIANG Xi-shu, XIE Bing. Novel recycle technology for recovering rare metals (Ga, In) from waste light-emitting diodes [J]. Journal of Hazardous Materials, 2015, 299: 388−394.

[13] DING Yun-ji, ZHANG Shen-gen, LIU Bo, ZHENG Huan-dong, CHANG Chein-chi, EKBERG C. Recovery of precious metals from electronic waste and spent catalysts: A review [J]. Resources, Conservation & Recycling, 2019, 141: 284−298.

[14] TUNCUK A, STAZI V, AKCIL A, YAZICI E Y, DEVECI H. Aqueous metal recovery techniques from e-scrap: Hydrometallurgy in recycling [J]. Minerals Engineering, 2012, 25(1): 28−37.

[15] NAGY S, BOKÁNYI L, GOMBKÖTŐ I, MAGYAR T. Recycling of gallium from end-of-life light emitting diodes [J]. Archives of Metallurgy and Materials, 2017, 62(2): 1161−1166.

[16] SWAIN B, MISHRA C, KANG L, PARK K S, LEE C G, HONG H S. Recycling process for recovery of gallium from GaN an E-waste of LED industry through ball milling, annealing and leaching [J]. Environmental Research, 2015, 138: 401−408.

[17] SWAIN B, MISHRA C, PARK K S, LEE C G, LEE K J, HONG H S. Recycling of GaN, a refractory eWaste material: Understanding the chemical thermodynamics [J]. International Journal of Applied Ceramic Technology, 2016, 13(2): 280−288.

[18] CHEN W S, HSU L L, WANG L P. Recycling the GaN waste from LED industry by pressurized leaching method [J]. Metals, 2018, 8(10): 861.

[19] MAAREFVAND M, SHEIBANI S, RASHCHI F. Recovery of gallium from waste LEDs by oxidation and subsequent leaching [J]. Hydrometallurgy, 2020, 191: 105230.

[20] POURHOSSEIN F, MOUSAVI S M, BEOLCHINI F, LO MARTIRE M. Novel green hybrid acidic-cyanide bioleaching applied for high recovery of precious and critical metals from spent light emitting diode lamps [J]. Journal of Cleaner Production, 2021, 298: 126714.

[21] van den BOSSCHE A, VEREYCKEN W, VANDER HOOGERSTRAETE T, DEHAEN W, BINNEMANS K. Recovery of gallium, indium, and arsenic from semiconductors using tribromide ionic liquids [J]. ACS Sustainable Chemistry & Engineering, 2019, 7(17): 14451−14459.

[22] ZHAN Lu, WANG Zheng-yu, ZHANG Yong-liang, XU Zhen-ming. Recycling of metals (Ga, In, As and Ag) from waste light-emitting diodes in sub/supercritical ethanol [J]. Resources, Conservation & Recycling, 2020, 155: 104695.

[23] KUMAR A, KUPPUSAMY V K, HOLUSZKO M, SONG S L, LOSCHIAVO A. LED lamps waste in Canada: Generation and characterization [J]. Resources, Conservation & Recycling, 2019, 146: 329−336.

[24] ZHAO Zhuo, YANG Yong-xiang, XIAO Yan-ping, FAN You-qi. Recovery of gallium from Bayer liquor: A review [J]. Hydrometallurgy, 2012, 125: 115−124.

[25] RAO M D, SINGH K K, MORRISON C A, LOVE J B. Recycling copper and gold from e-waste by a two-stage leaching and solvent extraction process [J]. Separation and Purification Technology, 2021, 263: 118400.

[26] LIU Wei, XU Jia-qi, HAN Jun-wei, JIAO Fen, QIN Wen-qing, LI Zhu-zhang. Kinetic and mechanism studies on pyrolysis of printed circuit boards in the absence and presence of copper [J]. ACS Sustainable Chemistry & Engineering, 2019, 7(2): 1879−1889.

[27] LIU Wei, ZHONG Xue-hu, HAN Jun-wei, QIN Wen-qing, LIU Tong, ZHAO Chun-xiao, CHANG Zi-yong. Kinetic study and pyrolysis behaviors of spent $LiFePO_4$ batteries [J]. ACS Sustainable Chemistry & Engineering, 2019, 7(1): 1289−1299.

[28] ZHONG Xue-hu, LIU Wei, HAN Jun-wei, JIAO Fen, QIN Wen-qing, LIU Tong, ZHAO Chun-xiao. Pyrolysis and physical separation for the recovery of spent $LiFePO_4$ batteries [J]. Waste Management, 2019, 89: 83−93.

[29] AHMADI A, REZAEI M, SADEGHIEH S M. Interaction effects of flotation reagents for SAG mill reject of copper sulphide ore using response surface methodology [J]. Transactions of Nonferrous Metals Society of China, 2021, 31: 792−806.

[30] SHAHNAZI A, FIROOZI S, HAGHSHENAS FATMEHSARI D. Selective leaching of arsenic from copper converter flue dust by Na_2S and its stabilization with $Fe_2(SO_4)_3$ [J]. Transactions of Nonferrous Metals Society of China, 2020, 30: 1674−1686.

[31] HOU Wen-yuan, LI He-song, LI Mao, CHEN Ben-jun, FENG Yuan. Effects of electrolysis process parameters on alumina dissolution and their optimization [J]. Transactions of Nonferrous Metals Society of China, 2020, 30: 3390−3403.

[32] WANG Li-min, ZHANG Guo-cheng, MA Fei. A study on comprehensive recycling of waste diamond tools [J]. Rare Metals, 2012, 31(1): 88−91.

[33] JAVED U, FAROOQ R, SHEHZAD F, KHAN Z. Optimization of HNO_3 leaching of copper from old AMD Athlon processors using response surface methodology [J]. Journal of Environmental Management, 2018, 211: 22−27.

[34] SUN P P, RHOB J, CHO S Y. Recovery of silver from the nitrate leaching solution of the spent Ag/α-Al_2O_3 catalyst by solvent extraction [J]. Industrial & Engineering Chemistry Research, 2014, 53(52): 20241−20246.

[35] SHAO Shuang, MA Bao-zhong, WANG Xin, ZHANG Wen-jun, CHEN Yong-qiang, WANG Cheng-yan. Nitric acid pressure leaching of limonitic laterite ores: Regeneration of HNO_3 and simultaneous synthesis of fibrous $CaSO_4·2H_2O$ by-products [J]. Journal of Central South University, 2020, 27: 3249−3258.

[36] MASLOBOEVA S M, ARUTYUNYAN L G, PALATNIKOV M N, MANUKOVSKAYA D V. Separation and purification of tantalum from plumbomicrolite of amazonite deposit in

Kola Peninsula by acid leaching and solvent extraction [J]. Journal of Central South University, 2021, 28: 72−88.
[37] LI Liang-yu, HAN Jun-wei, JIAO Fen, LIU Wei, QIN Wen-qing. High-efficiency hydrometallurgical separation of valuable components from waste alloy cutters [J]. The Chinese Journal of Nonferrous Metals, 2022, 32(4): 1098−1110. (in Chinese)

响应曲面法优化从废旧 LED 中浸出有价金属

魏徐一[1]，高永峰[2]，韩俊伟[1,2]，王勇伟[1]，覃文庆[1]

1. 中南大学 资源加工与生物工程学院，长沙 410083；
2. Department of Chemical and Materials Engineering, University of Alberta, Edmonton T6G 1H9, Canada

摘　要：通过热解和浸出工艺从废旧发光二极管(LEDs)中回收有价金属。通过对热解后的 LED 预先筛分可回收 98.16% Ga 和 99.54% Y。采用单因素试验和响应曲面法研究不同浸出条件对铁、铜和银浸出的影响。利用无氧化剂 H_2SO_4 浸出法从废旧 LED 中选择性回收约 90.15% Fe，Fe 浸出渣通过添加 HNO_3 浸出可以回收 99.55% Cu 和 99.36% Ag。XRD 和 SEM−EDS 分析证实，所开发的工艺可以高效地从废旧 LED 中浸出 Fe 和 Cu。

关键词：酸浸；金属回收；响应曲面法；废旧发光二极管

(Edited by Xiang-qun LI)